Ultrasonic Shear Wave Attenuation in Superconducting Tin*

J. R. LEIBOWITZ
Westinghouse Research Laboratories, Pittsburgh, Pennsylvania
(Received 14 August 1963)

The superconducting attenuation of transverse ultrasonic waves was studied experimentally in single crystal tin. The "residual" attenuation was found to be consistent with the relation $\alpha_s/\alpha_n \propto \exp(-\mathcal{E}/kT)$ at low reduced temperatures in tin; α_s/α_n is the superconducting-to-normal attenuation ratio and $\mathcal{E}$ is the superconducting energy gap. This functional form satisfied the low-temperature observations for all principal propagation and polarization orientations. Anisotropy in the apparent superconducting energy gap was demonstrated. It was found that anisotropy can be associated with polarization orientation as well as propagation orientation of the transverse lattice waves. Observed values of total and residual shear wave attenuation were found to suggest the importance of shear deformation interactions between the electron system and lattice waves in tin.

I. INTRODUCTION

THE theory of superconductivity of Bardeen, Cooper, and Schrieffer[1] (hereafter BCS) has been remarkably successful in accounting for most of the basic experimental features of superconductors.[2] The agreement of BCS predictions with experiment is especially impressive in view of the fact that a single isotropic energy gap was used to facilitate calculations from the theory. As has been noted by Cooper,[3,4] many of the qualitative features of superconductivity can be explained without a consideration of the details of the structure of metals. Hence, the theory based on an isotropic model of the metal is able to account for the main features of observed superconductive behavior, even though most of the metals which become superconductors have very complicated electronic band structure.

However,[2,5] apparent disagreements with the BCS theory exist which may in some instances be due to the simplifying assumption of isotropic superconducting properties in k space (see later). This possibility was discussed as early as 1958 by a number of conferees at the International Conference on the Electronic Properties of Metals at Low Temperatures, Geneva, New York, 25–29 August 1958 (unpublished). It has been realized, for example, that anisotropy in the energy gap could explain some of the anomalous experimental data on specific heats.[5,6] Near the superconducting transition temperature T_c the temperature dependence of the specific heat would be determined by some "average value" of the energy gap; as temperature is reduced from T_c, the smaller gaps become increasingly important in the weighted average since the energy gap appears exponentially in the specific heat.

The present work is concerned with an examination of the electron-shear wave interaction in superconducting tin and anisotropy in the superconducting energy gap, from measurements of the attenuation of transverse ultrasonic waves. Most transport processes depending on electron-lattice interaction involve the integrated interaction between the entire thermal vibrational spectrum and electron distribution. The power of the ultrasonic method for the examination of anisotropy in the electron-lattice interaction lies in the fact that, when $ql>1$, only those electrons which lie on a particular portion of the Fermi surface interact significantly with a given lattice wave; q is the wave number of the sound wave and l is the electron mean free path. Hence, measurements of ultrasonic attenuation as a function of crystallographic orientation should reflect anisotropies in the interaction with the electron distribution, and consequently demonstrate anisotropy of the superconducting energy gap. Anisotropy in the superconducting energy gap of tin has already been investigated by means of observations of the attenuation of longitudinal ultrasonic waves.[7,8] However, it is to be expected, at least on the free-electron model, that transverse lattice waves interact even more selectively with electrons on the Fermi surface. Observations of transverse lattice wave attenuation by electrons may, therefore, permit a more sensitive exploration of energy-gap anisotropy, and hence, in principle, improve the chances for establishing empirical connections between superconducting energy gap variation in k space and the associated Fermi surface topology. This objective is perhaps overly ambitious at present. As Bardeen[9] has noted, however, it is one which may be expected to provoke increasing attention, theoretically and experimentally.

Attenuation of ultrasound by electrons was first

* This work was derived in part from portions of a dissertation submitted in partial fulfillment of the requirements for the degree of Doctor of Philosophy at Brown University, 1962.

[1] J. Bardeen, L. N. Cooper, and J. R. Schrieffer, Phys. Rev. **108**, 1175 (1957).

[2] J. Bardeen and J. R. Schrieffer, in *Progress in Low Temperature Physics*, edited by C. J. Gorter (North-Holland Publishing Company, Amsterdam, 1961), Vol. III, p. 170.

[3] L. N. Cooper, Am. J. Phys. **28**, 91 (1960).

[4] L. N. Cooper, Summer Institute in Theoretical Physics, Brandeis University, 1959 (unpublished).

[5] L. N. Cooper, Phys. Rev. Letters **3**, 17 (1959).

[6] H. A. Boorse, Phys. Rev. Letters **2**, 391 (1959).

[7] R. W. Morse, T. Olsen, and J. D. Gavenda, Phys. Rev. Letters **3**, 15 (1959).

[8] P. O. Bezuglyi, A. A. Galkin, and A. P. Karolyuk Zh. Eksperim. i Teor. Fiz. **39**, 7 (1960) [translation: Soviet Phys.—JETP **12**, 4 (1961)].

[9] J. Bardeen, in Eighth International Conference on Low Temperature Physics, London, 1962 (to be published).

observed by Bömmel[10] in 1954, and soon after, independently, by Mackinnon.[11] Ultrasonic attenuation arising from electron-lattice interaction is strictly a low-temperature phenomenon because the interaction is significant only for electron mean-free-path l, such that $l\sim\lambda$, i.e., for $ql\sim 1$, where $q=2\pi/\lambda$ and λ is the sound wavelength. With conventional ultrasonic techniques this condition usually requires very pure metals and liquid-helium temperatures. Ultrasonic attenuation by electrons in metals has been examined theoretically by a number of workers. (For a review see Ref. 12.) For the case of longitudinal waves in the limit $ql\gg 1$, the problem has been treated by quantum theory as an example of electron-phonon scattering.[12,13] An ultrasonic wave can be made experimentally to approximate a plane harmonic lattice wave, which represents a perturbing potential V to the conduction electrons. Thus electrons are scattered, and the rate of energy transfer from a given lattice mode to the electron system is obtained from calculation of the net rate of phonon scattering $\partial n/\partial t$ due to all the conduction electrons. This entails a determination of the matrix element $\langle \mathbf{k}', n\pm 1 \,|\, V \,|\, \mathbf{k}, n\rangle$, describing the scattering of electrons from $\mathbf{k}$ to $\mathbf{k}'$ with simultaneous emission or absorption of a phonon initially in state n.

It is found that the only electrons on the Fermi surface appreciably scattered are those which, in the direction of the wave vector $\mathbf{q}$, have a component of group velocity equal to the sound speed u_s. This condition defines the so-called "effective zones," the regions of the Fermi surface on which the electrons move essentially in phase with the sound wave. In free-electron theory, electrons satisfying this condition lie on a band in the region of intersection of the Fermi sphere with the equatorial plane normal to $\mathbf{q}$, since $u_s/v_g\sim 10^{-3}$, typically, in a metal. Semiclassical calculations of the attenuation attributable to electron-phonon interaction have demonstrated a similar selectivity, when $ql>1$, in both the longitudinal and the transverse wave case. Morse[14] and Mason[15] obtained expressions for the attenuation of longitudinal and shear waves in the limiting case $ql<1$. Soon after, Pippard[16] presented a semiclassical treatment for the entire range of ql which agreed with the earlier predictions in the appropriate limits. We shall have occasion later to refer to Pippard's result for the transverse wave attenuation by electrons

$$\alpha=(Nm/\rho u_t\tau)(1-g/g), \tag{1}$$

where

$$g=\frac{3}{2(ql)^2}\left[\frac{(ql)^2+1}{ql}\tan^{-1}ql-1\right],$$

ρ is the density of the metal, τ is the relaxation time, and u_t is the shear wave velocity.

When the quantum-mechanical electron-phonon calculation for α is modified by the introduction of the superconducting density of states and by a coherence factor inherent in the BCS theory, the following result is obtained by BCS[1]:

$$\frac{\alpha_s}{\alpha_n}=2F(\mathcal{E})=\frac{2}{e^{\mathcal{E}(T)/kT}+1}. \tag{2}$$

That is, the ratio of the superconducting-to-normal attenuation, α_s/α_n, equals twice the Fermi function F of the temperature-dependent superconducting energy gap, $2\mathcal{E}$. Morse and Bohm[17] examined this prediction empirically and found the temperature dependence of longitudinal ultrasonic wave attenuation to be in reasonable agreement with Eq. (2), as have subsequent measurements by a number of observers.[8,18] The BCS expression for α_s/α_n, given by Eq. (2), was derived for the case of longitudinal waves, in the limit $ql>1$. Also, there was made the simplifying assumption that the BCS electron-electron interaction $V_{kk'}$ is constant in k space. Tsuneto[19] has indicated that the BCS expression should also remain valid, in the case of longitudinal waves, over the whole range of ql. It remains to consider further the isotropy assumption and the limitation to longitudinal waves. Concerning the former question, it has been pointed out by Cooper[5] that anisotropy in the energy gap of a superconductor is consistent with the framework of the theory. The appropriate BCS electron-electron interaction must in general be regarded as anisotropic in k space, and a result of the generalization is that the energy gap now becomes a function of $\mathbf{k}$ as well as T. It has already been noted that, when $ql>1$, the interaction of a longitudinal lattice wave with the electrons in a metal favors that group of electrons whose component of velocity $\mathbf{v}$ in the direction of the wave propagation vector $\mathbf{q}$ is equal to the sound speed u_s. By propagating ultrasound along different crystalline directions it then becomes possible to look for anisotropy of the superconducting energy gap. Morse, Olsen, and Gavenda[7] have demonstrated this feature of the longitudinal wave interaction with electrons in a superconductor.

We have also noted the original restriction of the BCS relation for α_s/α_n to the case of longitudinal waves. Experimental results for shear waves suggest a more complicated behavior than for longitudinal waves.[12] In general, the observed behavior of the shear wave attenuation as a function of temperature has been found to be roughly separable into two distinct regions (see Fig. 1). One of these is characterized by an initial very sharp drop in attenuation near T_c; the other, the so-called

[10] H. E. Bommel, Phys. Rev. **96**, 220 (1954).
[11] L. Mackinnon, Phys. Rev. **98**, 1181, 1210 (1955).
[12] R. W. Morse, *Progress in Cryogenics* (Heywood and Company Ltd., London, 1959), Vol. I.
[13] C. Kittel, Acta Met. **3**, 295 (1955).
[14] R. W. Morse, Phys. Rev. **97**, 1716 (1955).
[15] W. P. Mason, Phys. Rev. **97**, 557 (1955).
[16] A. B. Pippard, Phil. Mag. **46**, 1104 (1955).
[17] R. W. Morse and H. V. Bohm, Phys. Rev. **108**, 1094 (1957).
[18] Eighth International Congress on Low Temperature Physics, London, 1962 (to be published).
[19] T. Tsuneto, Phys. Rev. **121**, 402 (1961).

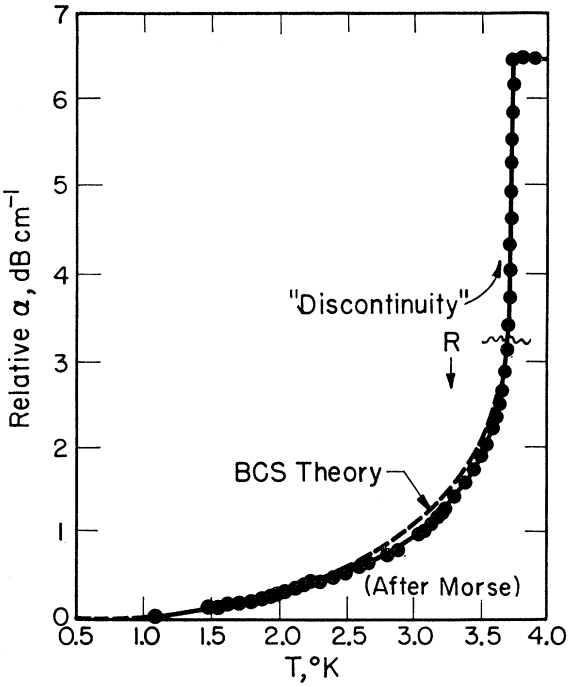

FIG. 1. Observed shear wave attenuation in a polycrystalline sample of tin at 27.5 Mc/sec. The BCS theory is compared with that part of the attenuation labeled R.

"residual" attenuation, indicated by "R" in the figure, is manifested as a more gradual falloff of α_s/α_n with temperature. The form of the residual shear wave attenuation, in common with that of longitudinal waves, appears to be in reasonable agreement with the BCS prediction, Eq. 2. In Fig. 1 the residual attenuation is compared with the BCS prediction for the case of 27.5-Mc/sec transverse-ultrasonic waves in polycrystalline tin.[12]

In the present study, some aspects of which have already been reported,[20] the shear-wave residual-superconducting attenuation, $\alpha_r(T)$ (the attenuation in the region labeled "R" in Fig. 1), was studied experimentally in tin. The experimental program included measurement of the magnitude of the residual electronic attenuation, $\alpha_r(T)$, as a function of shear wave orientation; observation of the dependence of the functional form of $\alpha_r(T)$ on orientation of propagation vector $\mathbf{q}$ and polarization vector $\boldsymbol{\varepsilon}$; and measurements to determine whether anisotropy in the apparent superconducting energy gap can be associated with the polarization orientation, as well as the propagation orientation, of the ultrasonic wave.

II. EXPERIMENTAL PROCEDURES

The measurements, made at liquid-helium temperatures as a function of temperature and crystalline orientation, involve observations on the spatial decay of ultrasonic pulses which have passed through the specimen under study. The pulses are excited by a quartz piezoelectric transducer, and received either at a second transducer at the opposite parallel face or as an echo at the first surface. The latter method was used exclusively in the present experiments. A sinusoidal-voltage pulse of several hundred volts is applied to the transducer, the center frequency of the pulse being tuned to a resonant frequency of the transducer. It is required that the material bonding the transducer to the sample provide acoustic contact between them, and this requirement presents considerable difficulty at liquid-helium temperatures. In the experiments to be described, frequencies of 30 to 70 Mc/sec and a pulse length of 1 μsec were employed.

The two single-crystal samples of tin used in these studies were grown from 99.9999% pure zone-refined tin (provided by the Vulcan Detinning Company) by the Czochralski method. The crystals were in the form of right circular cylinders, each having a pair of (001) planes at the ends. In addition, another pair of planes was cut in the side of each crystal; in one sample these were (100) planes and in the other way they were (110) planes. The two crystals had been cut from adjacent regions of the same original crystal. The samples were x-rayed by the back-reflection Laue technique in order to identify the pairs of planes and to estimate the accuracy of their orientation and parallelism. It was found that, for all surfaces, corresponding pairs of planes were oriented with respect to their principal lattice planes to within about 1°. The distance between planes for all sets of faces in the two samples was 1.19 cm. It should be noted that, in order to optimize the signal received at the transducer, the wave front of the lattice wave must be "in phase" with the receiving transducer surface. Hence the samples were hand lapped and etched until the surfaces were plane and parallel within 0.0001 inch over the area of the transducer face. Since the frequency at which most of the measurements were taken (50 Mc/sec) corresponds to a wavelength of approximately 0.002 in. for shear waves in tin, requirements with regard to flatness and parallelism were reasonably well satisfied.

The attenuation unit used for measurement of the attenuation of pulsed ultrasound will be described only in outline, since it has already been reported in detail in a number of places.[12,21–23] The electronic equipment included a rf pulsed oscillator for generating electrical pulses at the transducer surface, and superheterodyne receiver for detecting and amplifying the received signal. In order to measure the attenuation of successive echoes the time-delayed output of a calibrated pulse

[20] J. R. Leibowitz and R. W. Morse, Bull. Am. Phys. Soc. 7, 63 (1962); J. R. Leibowitz, Ph.D. thesis, Brown University, 1962 (unpublished).

[21] B. B. Chick, M.S. thesis, Brown University, 1953 (unpublished).

[22] R. L. Roderick and R. Truell, J. Appl. Phys. 23, 267 (1962).

[23] B. Chick, G. Anderson, and R. Truell, J. Acoust. Soc. Am. 32, 186 (1960).

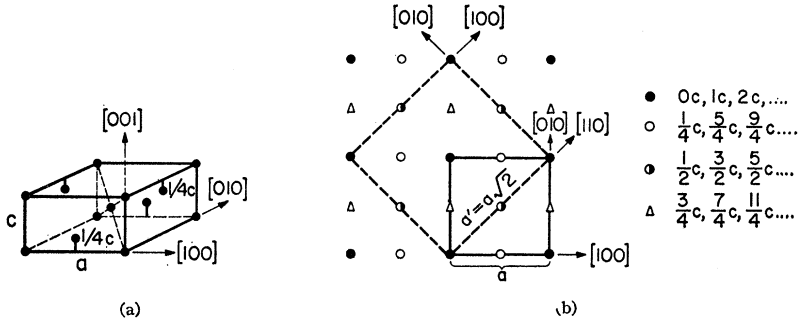

FIG. 2. The crystalline lattice of tin (after Olsen). (a) The standard representation of the tin lattice. $a=5.84\times10^{-8}$cm. $c=3.15+10^{-8}$cm. (b) The same lattice projected on a plane perpendicular to the [001] direction (or c—axis). The solid lines show the same cut of the lattice as does Fig. 2(a). The dash lines show the alternate (and rarely used) description of the lattice.

comparator was sent into the front end of the receiver. It was thus possible simultaneously to display an interlaced-comparator pulse and pulse-echo train. The horizontal sweep of the oscilloscope was actuated by a trigger pulse at the rate of 200/sec. These pulses also went to a switching circuit which caused the pulsed oscillator and the pulse comparator to be triggered alternately. Hence, the horizontal sweep was synchronized with the excitations from the pulsed oscillator and the pulse comparator, both of which were triggered at a rate of 100/sec. The pulsed oscillator output excited the quartz crystal, which in turn caused an elastic wave to be generated in the sample. The received pulse, along with a calibrated comparator pulse, was put into the mixer together with the signal from the local oscillator. The signal was amplified and detected in a 60-Mc/sec i.f. strip and the amplified signal applied to the vertical plates of the oscilloscope, which displayed the successive echoes of the elastic wave in the sample. The calibrated comparator pulse, matched to a given signal pulse, was used to measure the attenuation as a function of temperature.

III. EXPERIMENTAL RESULTS AND ANALYSIS

A. Temperature Dependence of the Attenuation

The superconducting-to-normal attenuation ratio, α_s/α_n, for transverse-ultrasonic waves was measured as a function of temperature for all principal propagation directions and all corresponding polarization orientations permitted by the elastic symmetry. The crystalline lattice of tin[24] may be represented as in Fig. 2. Since tin is tetragonal, propagation vectors were chosen along the [001] direction (the c axis) and the [100] direction (the a axis), having fourfold and twofold rotational symmetry, respectively. The tetragonal structure of tin permits the examination of the effect of polarization vector orientation for fixed $\mathbf{q}$, as follows: When $\mathbf{q}$ is parallel to the dyad axis, [100], two distinct polarization orientations are possible, namely $\boldsymbol{\epsilon}$ along [010] and along [001]; for propagation along [001] all polarization directions normal to $\mathbf{q}$ are elastically degenerate, due to the fourfold rotational symmetry about [001]. Nevertheless, the temperature dependence of superconductive attenuation was also observed for a range of polarization orientations about the axis.

The temperature dependence of attenuation in the "residual" region (recall Fig. 1) was examined in detail at low reduced temperatures, $t(t=T/T_c)$, viz., from the region of the lambda point to approximately 1.2°K. The validity of the approximation

$$\alpha_s/\alpha_n=2(e^{\mathcal{E}(T)/kT}+1)^{-1}=2e^{-\mathcal{E}(T)/kT}$$

may be assumed at temperatures such that $e^{\mathcal{E}/kT}\gg1$. From Appendix A, which was obtained from a numerical solution[25] of the BCS integral equation for $\mathcal{E}(T)$, the condition $e^{\mathcal{E}/kT}\gg1$ is seen to be amply satisfied for $T_c/T>1.7$. Also, it is seen that $\mathcal{E}$ is not sensibly temperature-dependent in the same region: for $T_c/T=2$, $2\mathcal{E}(t)$ differs from $2\mathcal{E}(0)$ by about $0.1\ kT_c$. Such a small deviation at the lower values of T_c/T will be seen to have no measurable effect in the final graphical determination of the value of $2\mathcal{E}(0)$; and, of course, $\mathcal{E}(t)$ approaches even closer to $\mathcal{E}(0)$ as T_c/T increases. The attenuation in this temperature region may, then, be written in the form

$$\ln(\alpha_s/\alpha_n)=K-X(T_c/T),$$

where $2X=2\mathcal{E}/kT_c$, the energy gap in units of kT_c, is essentially temperature-independent. Further, in the

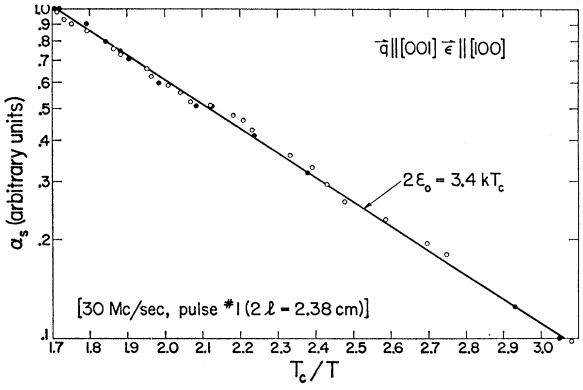

FIG. 3. The superconducting attenuation at low reduced temperatures for propagation along [001]. The solid and the open circles represent independent experiments.

[24] T. Olsen, in *The Fermi Surface*, edited by W. A. Harrison and M. B. Webb (John Wiley & Sons, Inc., New York, 1960), p. 237.

[25] The calculation was programmed by M. T. Thomas, of the Department of Physics, Brown University.

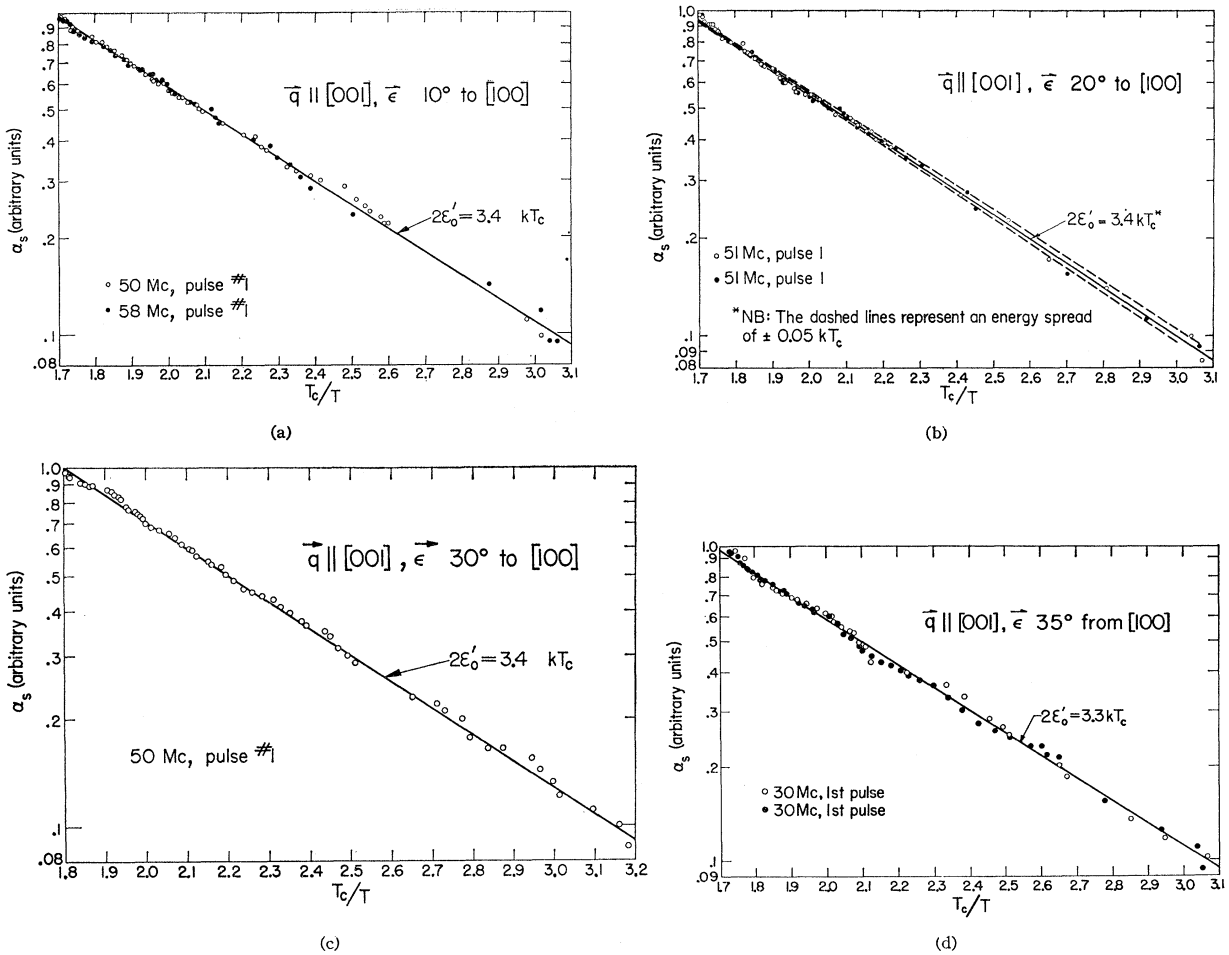

FIG. 4 (a)-(d). The superconducting attenuation at low reduced temperatures for propagation along [001] and ϵ rotated in the (001) plane.

temperature range with which we are here especially concerned, the temperature dependence of the attenuation resides only in the quantity α_s; in the ultrasonic attenuation measurements at the frequencies employed in these experiments (30–70 Mc/sec) there is no detectable temperature dependence of α_n in this range of temperatures. This is in keeping with the observations of Morse and Bohm,[17] and Morse, Olsen and Gavenda.[7] To test consistency with the BCS relation, attenuation was measured as a function of temperature and $\ln(\alpha_s/\alpha_n)$ plotted versus T_c/T to determine whether the resultant curves in the region $T_c/T>1.7$ were of linear form, within the limits of experimental error.

In Figs. 3 and 4 are shown representative data. These figures refer to propagation along the [001] axis and shear polarization vector rotated in the (001) plane through the indicated angles, measured from the [100] direction. Since these particular orientations are all elastically equivalent, the data permit a test of internal consistency of the method. It has already been shown that, for present purposes, the important temperature range lies below about 2.2°K, which, since $T_c=3.72$°K for tin, corresponds to a T_c/T value of about 1.7. Hence, to facilitate an examination of the temperature dependence of the attenuation, abscissas have been expanded to cover essentially this T_c/T range, and ordinates normalized by setting equal to one the corresponding attenuation change (typically, for **q** along [001], about 1.0 and 1.8 dB/cm at 30 Mc/sec and 50 Mc/sec, respectively). The expanded and normalized scales for $\ln(\alpha_s/\alpha_n)$ versus T_c/T permit a detailed examination of the form of the function. Fig. 3 shows two independent results for the same orientation, **q** along [001] and **ε** parallel to [100]. In Figs. 4(a)–(d) are shown similar graphical representations for other elastically equivalent orientations, as indicated.

In determining the functional form of $\ln(\alpha_s/\alpha_n)$ versus T_c/T in the region of interest, it is necessary to isolate the nonelectronic attenuation. Electronic attenuation in the superconducting state is expected on theoretical grounds to fall steadily from its value at T_c until at 0°K it disappears entirely, leaving only the

nonelectronic sources of ultrasonic attenuation. In order to determine the zero of electronic attenuation, which serves as a reference for the electronic attenuation measured at finite temperatures, it is necessary to extrapolate the measured attenuation from its value at 1.1°K. It must be assumed that the extrapolation, $\delta\alpha_0$, introduces an error in the estimate of the true electronic attenuation. It should be noted that the $\delta\alpha_0$ values which are found to linearize the data plots are consistent with those predicted from the BCS relation, Eq. (2); the agreement between the predicted extrapolation and that observed to linearize the data lies well within the experimental limiting scatter.[26] It is clear, of course, that such an experimental examination does not point uniquely to a functional form for $\alpha_s(T)$, but, rather, provides an empirical test for consistency of the BCS relation with the experimental observations. It is concluded that, in pure single crystal tin at low reduced temperatures ($t\approx 0.3$ to 0.6), α_s/α_n for transverse waves is consistent with the relation

$$\alpha_s/\alpha_n \propto e^{-\varepsilon/kT},$$

in agreement with BCS.

B. Selectivity of the Shear Wave Interaction

The free-electron model. To demonstrate the selectivity of the transverse wave interaction with free electrons it is useful to adopt a result obtained by Holstein[27] in treating ultrasonic attenuation by free electrons using the Boltzmann transport equation. The sound wave is associated with an ion density modulation in the longitudinal-wave case and a lattice-ion current in the case of transverse waves. There is established a quasi-neutrality of the combined electron and ion density modulations for the compressional modes and, at frequencies below $\sim 10^9$ sec^{-1}, a quasibalance of the combined transverse electron and lattice ion currents for the case of the transverse modes. In the solution of the Boltzmann equation for the perturbed-distribution function f, the electron-velocity distribution is given as a function of the velocity amplitude of the lattice vibration $\mathbf{u}_0$ and the local electric field associated with the sound wave.

It is assumed that scattering is by impurities, and that "collision drag"[27,28] causes the electrons to relax toward a Fermi distribution centered not at zero velocity but at the local lattice velocity accompanying the wave. It is found that Φ, the perturbation of the distribution from f_0, the equilibrium Fermi distribution in the absence of the sound wave (viz, $\Phi=f-f_0$), is given by

$$\Phi=-\frac{[m\mathbf{u}\cdot\mathbf{v}-e\mathbf{E}\cdot\mathbf{v}\tau+\frac{2}{3}(\zeta_0/N)j_L/u_s]\partial f_0/\partial\beta}{1+i\omega\tau[(v_x/u_s)-1]}. \quad (3)$$

Here $\mathbf{u}$ and $\mathbf{E}$ are the local lattice velocity and electric field, respectively, associated with the wave; $\mathbf{v}$ is the electron velocity; τ is the relaxation time; ζ_0 and N are the undisturbed (equilibrium) Fermi energy and electron density, respectively; u_s is the velocity of sound; j_L is the current (equal to zero for the case of transverse waves) associated with the dynamical separation of charges (ions and electrons) arising from the passage of a lattice wave having angular frequency ω; and β is the electron energy measured from the Fermi surface.

This expression for Φ, the perturbed part of the Fermi distribution of electrons, can be used to demonstrate explicitly the properties of selectivity identifiable in the interaction of the lattice wave with the free electrons. Since u, E, and j_L all have a wave-like dependence expressible by $e^{i(kx-\omega t)}\equiv e^{i\theta}$, we may write

$$\mathrm{Re}\Phi=-(\partial f_0/\partial\beta)PR\{\cos\theta+\omega\tau[(v_x/u_s)-1]\sin\theta\}, \quad (4)$$

where, for convenience, we have written

$$P\equiv\{1+(\omega\tau)^2[(v_x/u_s)-1]^2\}^{-1} \quad (5)$$

and

$$R\equiv[m\mathbf{v}\cdot\mathbf{u}_0-e\mathbf{v}\cdot\mathbf{E}_0\tau+\tfrac{2}{3}(\zeta_0/Nu_s)j_L]. \quad (6)$$

The following observations may be made from Eqs. (4)–(6). The factor $[-(\partial f_0/\partial\beta)]$ in Eq. (4) is essentially of the form of a delta function. Its presence indicates that Φ peaks at the Fermi surface, as is, of course, required. The last factor is simply a phase factor multiplying the entire expression, and is not relevant for present considerations. Consider now the remaining factors.

It is to be noted from Eq. (5) that Re Φ is a maximum when $u_s=v_x$. This result, of course, pertains both to longitudinal and shear waves, and demonstrates that maximum attenuation is to be associated with the condition $u_s=v_x$, as was noted in Chap. I. It is also evident that the sharpness of the perturbed region—and, hence, of the electron-phonon selectivity—is enhanced with increase of ql. This can be seen most simply as follows. Since $\omega\tau=ql(u_s/v_0)$ and $v_x=v_0\cos\phi$, where ϕ is the angle subtended by the electron velocity $\mathbf{v}_0$ and the propagation direction (the x axis), Eq. (5) may be rewritten

$$P(\phi)=[1+(ql/v_0)^2(v_0\cos\phi-u_s)^2]^{-1}.$$

It is seen that the amplitude of the perturbation falls to half-maximum when

$$\cos\phi=(u_s/v_0)+(1/ql).$$

Now $(u_s/v_0)\sim 10^{-3}$, while $(1/ql)$ lies in the range 10^{-1} to 10^{-2} in these experiments. Hence, for increasing values of ql, up to $ql=v_0/u_s$ (corresponding to frequencies

[26] Attenuation change was detectable to 0.1 dB, corresponding to an uncertainty in the determination of change in relative attenuation coefficient given by 0.1 dB/path length, or 0.04 dB/cm.

[27] T. Holstein, Research Memo 60–94 698-3-M17, Westinghouse Research Laboratories, Pittsburgh, Pennsylvania, 1956 (unpublished).

[28] T. Holstein, Phys. Rev. **113**, 479 (1959).

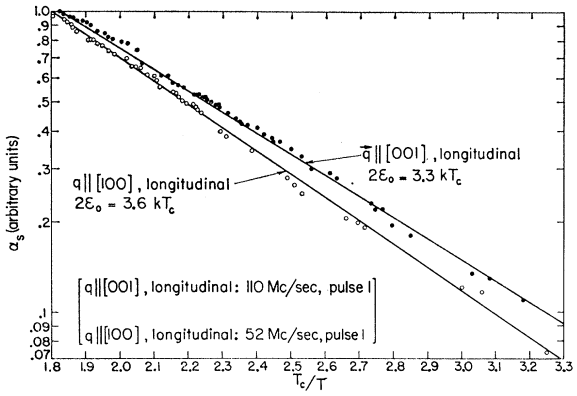

FIG. 5. Anisotropy of the temperature dependence of attenuation of longitudinal waves.

>1000 Mc/sec for the given tin samples), the perturbed region, or the effective zone, becomes more and more sharply localized in k space. The foregoing inferences refer equally well to the longitudinal and the shear wave interaction with electrons. The factor R, given by Eq. (6), has special meaning for the shear wave case, however. Since it is assumed in this treatment that $j_L=0$ for the shear wave case,

$$R(\text{shear})=(m\mathbf{u}_0-e\tau\mathbf{E}_0)\cdot\mathbf{v}.$$

Both $\mathbf{u}_0$ and $\mathbf{E}_0$, the velocity amplitude and amplitude of the electric field, now have the direction of the polarization vector of the lattice wave and can lead to contributions to Φ. The magnitude of R(shear) will be greatest when polarization orientation is along $\mathbf{v}$; the electrons on the edge of the "disk" (determined by the factor P) which interact especially strongly, are those having velocity $\mathbf{v}$ oriented along the direction specified by the polarization vector. Φ varies as $\cos\beta$, where β is the angle enclosed by the polarization direction and the velocity $\mathbf{v}$ of a given electron. On the free-electron model, then, the polarization orientation of shear waves exerts a selective effect in the electron-phonon interaction.

Evidence for anisotropy of the superconducting attenuation. Before treating the shear wave case, the longitudinal wave measurements reported by Morse,[7] and later by Bezuglyi,[8] were repeated as a check of consistency with the present work. The results are shown in Fig. 5. The superconducting energy gap values which have been reported in the literature for tin are summarized below. It is seen that the longitudinal wave energy gap values measured in the present work, and represented in Fig. 5, are in agreement with those of Morse *et al.*[7] Mackintosh's[29] tabulated measurements of shear-wave attenuation in superconducting tin suggest that anisotropy of the apparent energy gap is associated

TABLE I. Limiting energy gaps (in units of kT_c) observed with tin.

Source	Orientation of q [001]	[100]	]110]
Morse, Olsen and Gavenda[a] (longitudinal waves)	3.2±0.1	3.5±0.1	3.8±0.1
Mackintosh[b] (shear waves)	3.2±0.3	3.4±0.3	3.7±0.3

[a] See Ref. 7.
[b] See Ref. 29.

with propagation orientation for shear waves also. Although there appears to be good agreement between the tabulated longitudinal and shear data, it is not certain, as has been noted by Morse,[30] that such a comparison is very meaningful since the shear wave interaction is expected to favor different groups of electrons; the effect of polarization vector orientation was not reported, and, as has already been seen, there is reason to expect that shear polarization orientation may affect the selectivity. For a fixed propagation direction, the apparent limiting energy gap (see Table I) was indeed found in the present work to depend on the orientation of the polarization vector.

As has already been noted, the tetragonal structure of tin permits an examination of the effect of polariza-

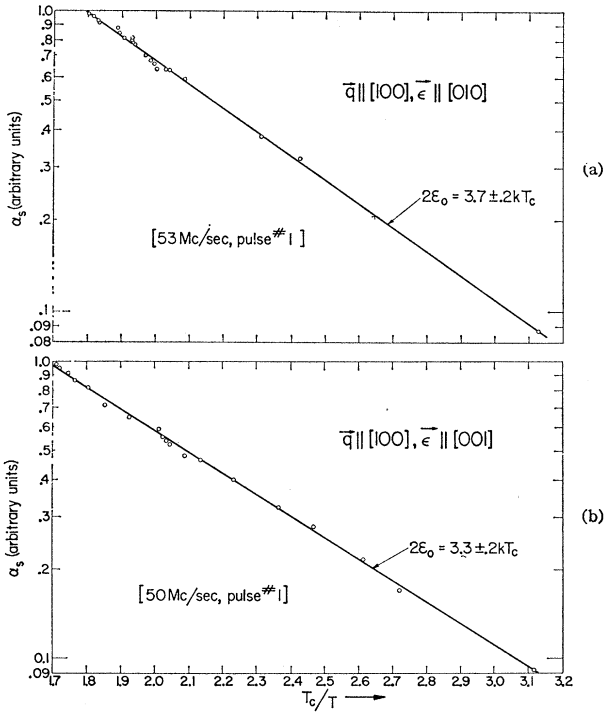

FIG. 6 (a)-(b). The superconducting attenuation at low reduced temperatures; anisotropy associated with shear polarization orientation.

[29] A. R. Mackintosh, in *Proceedings of the VII International Conference on Low Temperature Physics*, edited by G. M. Graham and A. C. H. Hallett (The University of Toronto Press, Toronto, 1961).

[30] R. W. Morse, in *Proceedings of the VII International Conference on Low Temperature Physics*, edited by G. M. Graham and A. C. H. Hallett (The University of Toronto Press, Toronto, 1961).

tion vector for fixed **q**. About the [100] axis there is a twofold rotational symmetry; for waves propagated along [100] the shear waves having polarization vectors oriented along [010] and [001] have different velocities. The two polarization orientations, then, are to be associated with distinct lattice modes. The results of these measurements are represented in Figs. 6(a) and 6(b). The apparent superconducting energy gaps corresponding to these two distinct polarization orientations are 3.7 ± 0.2 and $3.3\pm0.2\ kT_c$, for $\boldsymbol{\varepsilon}$ along the [010] and along the [001] axis, respectively. It is the latter number which must be compared with Mackintosh's result: Of the two polarizations associated with this **q** orientation, viz., **q** parallel to [100], the one examined by Mackintosh (private communication) corresponded to $\boldsymbol{\varepsilon}\|[001]$. Agreement is seen to be quite good.

In Figs. 7 and 8 are summarized the shear data relating to anisotropy in the superconducting energy gap. When the results represented by Fig. 6 are compared with those presented earlier for the orientation $\mathbf{q}\|[001]$ and $\boldsymbol{\varepsilon}\|[100]$ (see Fig. 3), it is possible to examine the energy gap anisotropy associated with the propagation vector **q** and with polarization vector $\boldsymbol{\varepsilon}$ of the shear lattice wave: Figure 7 shows the energy gap anisotropy associated with variation of **q** direction for fixed polarization orientation; in Fig. 8 it is seen that, although **q** has a fixed [100] orientation in both cases, a marked anisotropy in energy gap is experienced when $\boldsymbol{\varepsilon}$ is rotated about the dyad axis by 90°. Despite the orientational selectivity associated with the interaction between the transverse-ultrasonic wave and the electron system, the measured energy gaps must be regarded as reflecting some average value, the "weighting" of which is determined by the effective zones selected by the lattice wave. The Fermi surface of tin[24,31,32] may extend into the sixth Brillouin zone, and it is to be assumed that the effective zones in each sheet in k space contribute to the superconducting attenuation in a rather

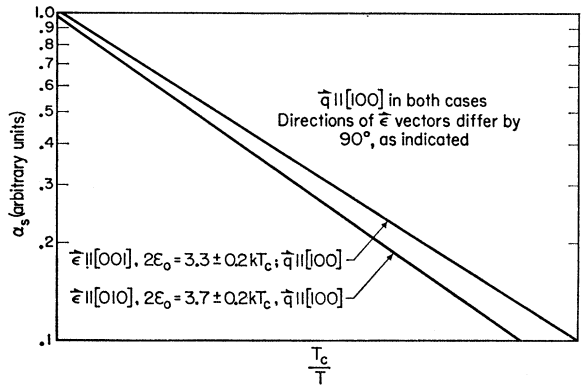

FIG. 7. Anisotropy in the superconducting energy gap; orientation dependence of gap on propagation vector **q**, for fixed $\boldsymbol{\epsilon}$.

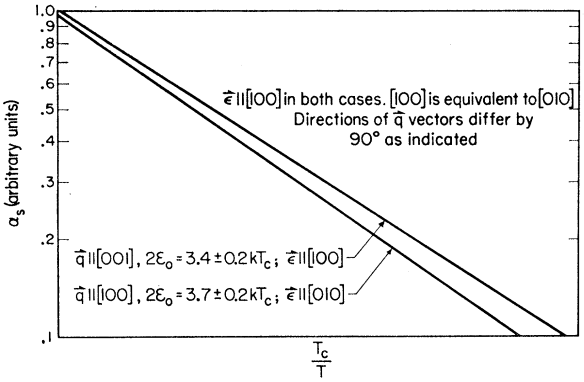

FIG. 8. Anisotropy in the superconducting energy gap: orientation dependence of gap on polarization vector $\boldsymbol{\epsilon}$, for fixed **q**.

complicated fashion. Thus, as Tinkham[33] has noted, such measurements set a lower bound on the anisotropy. The implications of such data, the relation between properties of a given Fermi surface and the gap anisotropy, are not well understood theoretically at present and have recently been the subject of some attention.[34,35]

At a given orientation, furthermore, it is possible, in principle, for different energy gaps to dominate in different temperature regions, owing to the exponential form of the temperature dependence. Cooper[5] has given a simple example of such an effect for the case of the superconducting electronic specific heat, the temperature dependence of which has a form similar to that of α_s/α_n at low temperatures. Given two energy gaps $\mathcal{E}_1$ and $\mathcal{E}_2$, the following form for the electronic specific heat will obtain at low temperatures:

$$\ln(C_{es}/\gamma T_c)\approx C+\tfrac{3}{2}\ln(T_c/T) +\ln[a_1\exp^{(-\mathcal{E}1/kT)}+a_2\exp^{(-\mathcal{E}2/kT)}],$$

where C_{es} is the electronic specific heat and C is a constant. Given $a_1>a_2$ and $\mathcal{E}_1>\mathcal{E}_2$, the second term in the bracket dominates in the region of large T_c/T, while the first term dominates at smaller values of T_c/T. This argument was originally employed to account for observations[2,6] on C_{es} which indicated that, when a sufficiently broad T_c/T range is examined, more than one exponential region generally seems to appear; when $\ln(C_{es}/\gamma T_c)$ is plotted versus T_c/T in the low temperature range ($T_c/T>1.5$), the curves, essentially straight lines at first, often develop an upward curvature in the region $T_c/T>3.5$. In reviewing the particular case of tin, Bardeen and Schrieffer[2] suggest that the development of an upward curvature at low reduced temperatures is evidence for an anisotropic energy gap in tin. The acoustic measurements obtained in the present

[31] A. V. Gold and M. G. Priestley, Phil. Mag. **5**, 1089 (1960).
[32] T. Olsen, J. Phys. Chem. Solids **24**, 649 (1963).
[33] M. Tinkham, in *Low Temperature Physics*, edited by C. DeWitt, B. Dreyfus, and P. G. de Gennes (Gordon and Breach, Inc., New York, 1962).
[34] V. L. Pokrovskii, Zh. Eksperim. i Teor. Fiz. **40**, 641 (1961) [translation: Soviet Phys.—JETP **13**, 447, 628 (1961)].
[35] I. A. Privorotskii, Zh. Eksperim. i Teor. Fiz. **42**, 450 (1962) [translation: Soviet Phys.—JETP **15**, 315 (1962)].

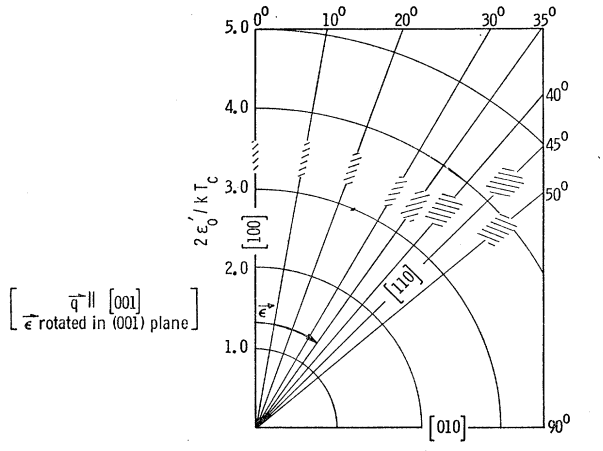

FIG. 9. Anisotropy of $\alpha(T)$ as a function of polarization vector orientation in the (001) plane. The hash marks represent both the experimental error associated with each determination of $\mathcal{E}'_0$ and the independent uncertainty in the polarization orientation of the shear transducer on the crystal surface.

work did not extend below temperatures corresponding to $T_c/T=3.2$; detailed observations relating to the gap measurements were confined to the range $T_c/T\approx1.7$ to 3.2. As was seen in Sec. (III.A), α_s/α_n is representable in this range by a single exponential for each orientation.

Rotation of polarization vector in the (001) plane. For propagation along [001] the attenuation should be independent of the plane of polarization, due to the symmetry properties of the crystal and the fact that the polarization is a tensor of only first rank: Because of the 90° rotational symmetry of the crystal, orthogonal polarization vectors $\boldsymbol{\varepsilon}_1$ and $\boldsymbol{\varepsilon}_2$ must be associated with the same velocity and attenuation coefficient; $\boldsymbol{\varepsilon}_1$ and $\boldsymbol{\varepsilon}_2$ define equivalent polarization directions for a lattice wave. Thus, one would expect the experimental results to be independent of the polarization vector for propagation along [001]. Nevertheless, measurements were made as a function of polarization direction for propagation along [001]. The angular variation of apparent energy gap is shown in Fig. 9. In all, there are 14 independent experimental runs involved here because most of the orientations were repeated. Fig. 9 shows that the variation of apparent energy gap with the direction of polarization is essentially independent of angle, the value being about $3.4kT_c$ except in the region of 45°, viz., the case $\boldsymbol{\varepsilon}$ along [110]. The hash marks represent both the experimental error associated with the determination of $\mathcal{E}_0'$ and the independent uncertainty in the polarization orientation of the shear transducer on the crystal surface. Under the conditions of the experiment the angular error increases with angle, measured from the reference edge (along [100]) of the crystal surface, and is estimated to be $\pm2°$ at the largest angle. The apparent variation of energy gap, corresponding to rotation of polarization vector in the (001) plane, appears to be associated with geometrical effects which give rise to an effective removal of the elastic degeneracy, as seen by the ultrasonic wave. For propagation along a fourfold axis of symmetry, it can be shown[36] that such wave interference effects are expected to be significant only when polarization lies, in the "fourfold" plane, essentially midway between principal axes. This is consistent with the observation that anomalous results associated with rotation of $\boldsymbol{\varepsilon}$ in the plane are confined to the region of 45° (see Fig. 9). These effects are not relevant to the present considerations, and are to be treated separately.

C. The Normal Attenuation

It is of interest to examine the total, or normal-state, electronic attenuation, α_n, which is measured by determining the attenuation difference between the extrapolated 0°K value and that corresponding to temperatures just above T_c; as was noted earlier, the nonelectronic attenuation in tin, in the frequency range treated in these measurements (10–50 Mc/sec), has no detectable dependence on temperature in the liquid helium range. The normal attenuation data are summarized in Table II. It is not surprising that these results are not consistent with the simple free-electron predictions, which would require that, for $ql>1$, the low-temperature normal-state attenuation for longitudinal waves, α_l, and for transverse waves, α_t, be given by[12]

$$\alpha_l=(\pi/6)NmV_0q/\rho u_l \tag{7}$$

and

$$\alpha_t=(4/3\pi)NmV_0q/\rho u_t; \tag{8}$$

V_0 is the magnitude of the Fermi velocity (a constant over the spherical Fermi surface), q is the wave number, and u_l and u_t are the magnitudes of the longitudinal and shear wave velocities, respectively. In order to facilitate a data comparison, the attenuation values tabulated in the last column, labeled "α_n (reduced)," have been scaled so as to correspond to equivalent attenuation values at frequencies of 30 or 10 Mc/sec, as indicated. In making the reduction it is assumed that $\alpha_n\propto\omega$. Use had been made here of the fact that both the free-electron results given by Eqs. (7) and (8) and the "real-metal" results of Pippard[37] (see later) require that α_n be proportional to ω, when $ql\gg1$. The linear approximation is probably justified only for the 30-Mc/sec shear wave data, for which the lower-limit estimate of ql is a ql value of 10. The estimated error in determination of reduced α_n values is ±1.0 and ±0.4 dB/cm for the 30 and the 10-Mc/sec data, respectively.

The normal attenuation results summarized in Table I give evidence for the inadequacy of a simple free-electron description of the attenuation for tin. Consider, for example, the longitudinal attenuation data. Equation (7) would dictate that the longitudinal attenuation have essentially the same value for both the [001] and

[36] P. C. Waterman and L. J. Teutonico, J. Appl. Phys. **28**, 266 (1957).
[37] A. B. Pippard, Proc. Roy. Soc. (London) **A257**, 165 (1960).

TABLE II. Measurements of the normal electronic attenuation α_n.

Sample	Orientation	Frequency (Mc/sec)	α_n (dB/cm)	α_n(reduced) (dB/cm)
I	$q\|\|[001]$, $\epsilon\|\|[100]$	34.0	15.1	13.3 (30 Mc/sec)
I	$q\|\|[001]$, $\epsilon\|\|[110]$	33.5	14.8	13.2 (30 Mc/sec)
II	$q\|\|[001]$, $\epsilon\|\|[100]$	31.0	13.6	13.2 (30 Mc/sec)
II	$q\|\|[001]$, ϵ 10° to [100]	11.4	4.1	3.6 (10 Mc/sec)
II	$q\|\|[001]$, ϵ 15° to [100]	10.8	3.8	3.5 (10 Mc/sec)
II	$q\|\|[001]$, ϵ 20° to [100]	10.6	3.6	3.4 (10 Mc/sec)
II	$q\|\|[100]$, $\epsilon\|\|[001]$	10.2	2.2	
II	$q\|\|[100]$, $\epsilon\|\|[010]$	10.3	3.3	
II	$q\|\|[110]$, $\epsilon\|\|[110]$	10.2	2.7	
II	$q\|\|[001]$, longitudinal	30.3	8.7	
II	$q\|\|[100]$, longitudinal	10.3	4.0	
II	$q\|\|[110]$, longitudinal	30.4	4.2	

the [110] orientation; it is to be noted from Appendix B[38] that the ratio of q values for the two orientations, at the indicated frequencies, is approximately unity. Similar comments apply to the relative attenuations for [100] and [110]: It is not possible to reconcile the fact that $\alpha_n[100]/\alpha_n[110]$ is essentially unity with the corresponding ratio of q values [see Appendix B], which is approximately $\frac{1}{3}$. Similar conclusions can be drawn from a comparison of Eq. (8) with the shear wave data summarized in Table II. The results corresponding to shear propagation along [100] demonstrate an anisotropy in the total attenuation for the two distinct polarization orientations which cannot be compensated by "q scaling."

The substitution of a more realistic model for the simple free electron one would, of course, be expected to modify the description of ultrasonic attenuation by electrons. In the past few years several attempts have been made to provide a theory for the interaction between an acoustic wave and an arbitrary Fermi surface.[37,39,40] The most detailed of these is perhaps that due to Pippard.[37] Pippard analyzes the forces acting on an electron, as viewed by an observer at rest in the lattice and at the position of the given electron. Apart from the electromagnetic forces, two additional effects appear. It must be assumed that the equilibrium shape of an arbitrary Fermi surface is strain-dependent. Moreover, as an electron travels from point to point in the metal, it experiences a change in the wave vector $\mathbf{k}$, as seen by the fixed observer, as a result of the relative velocity of different parts of the lattice. These effects are treated by the introduction of fictitious fields in the stationary undeformed lattice, and it is demonstrated that both give rise to dissipative effects when the strain is time-dependent. The attenuation is obtained by calculating the currents set up by the real and fictitious forces.

The results applicable to pure shear and pure longitudinal waves, in the limit $ql\gg1$, are of special interest here. These are as follows:

$$\alpha\sim\frac{\hbar q}{4\pi^2\rho u_s}\oint RD_x^2 d\psi \tag{9}$$

for the case of longitudinal waves in the lim $ql\gg1$; and

$$\alpha\sim\frac{\hbar q}{4\pi^2\rho u_s}\left[\oint RD_y^2 d\psi+\frac{1}{\pi^2}\frac{[\int D_y\tan\phi\cos\psi dS]^2}{\oint R\cos^2\psi d\psi}\right], \tag{10}$$

for the shear wave case in the limit $ql\gg1$. Propagation and shear polarization vectors are taken along the x axis and y axis, respectively. The line integrals are taken about the "effective zones," defined earlier as the loci of points on the Fermi surface for which $v_x\approx u_s$, viz., the regions for which $\phi\approx\pi/2$, since $u_s\ll v_0$. (It is recalled that in the free-electron treatment the interaction was confined essentially to the effective zone, when $ql\gg1$.) As before, ϕ is the angle subtended by the propagation vector $\mathbf{q}$ and the electron velocity $\mathbf{v}$; ψ represents angular measure about the effective zone. Finally, R is the reciprocal of the Gaussian curvature on the effective zone at a given point P, specified by ψ. The quantities D_x and D_y are components of a deformation tensor.

Equations (9) and (10) demonstrate in terms of the Gaussian curvature and deformation, the sources of the attenuation anisotropy reported earlier—albeit in the limiting case $ql\gg1$, for which the expressions are considerably simplified. The attenuation, as in the free-electron case, is independent of mean free path and is proportional to frequency. This result has already been used. Further, according to Eq. (9), the electrons which are important in the interaction with longitudinal waves are those lying in the "effective zones," again in agreement with the free-electron treatment. In the shear-wave case, as can be seen from Eq. (10), there is an

[38] J. A. Rayne and B. S. Chandrasekhar, Phys. Rev. **120**, 1658 (1960).
[39] E. I. Blount, Phys. Rev. **114**, 418 (1959).
[40] R. G. Chambers, in *Proceedings of the VII International Conference on Low Temperature Physics*, edited by G. M. Graham and A. C. H. Hallett (The University of Toronto Press, Toronto, 1961).

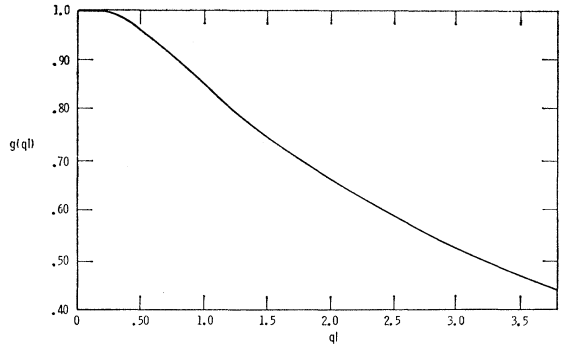

FIG. 10. The ql dependence of the function g.

additional contribution from an integral taken about the whole Fermi surface, even in the $ql \gg 1$ limit. It is seen from these expressions that it is possible, in principle, to relate experimentally observed normal-state attenuation anisotropy to the Gaussian curvature and deformation of the Fermi surface about the effective zones. It is also clear, however, that such studies can most fruitfully be performed in metals having relatively simple and well understood Fermi surfaces.

D. The Residual Superconducting Attenuation: Deformation Effects

It is of interest to ask whether consequences of the complexity of the tin Fermi surface cannot be demonstrated in the superconducting attenuation by electrons. The first Brillouin zone of tin can hold one electron/atom. The four valence electrons are accompanied by a free-electron sphere in k space which completely encloses the first Brillouin zone, and intersects Brillouin zone faces as far as the sixth Brillouin zone.[31] As a consequence, a number of very intricate sheets in k space make up the reduced-zone free-electron Fermi surface. Although the experimental evidence[41] does not appear to be consistent with the free-electron picture of the reduced-zone surfaces in very much detail, the data do indicate that the actual situation must be of the same degree of complexity. Deformation contributions to absorption of the acoustic wave are to be expected near regions of intersection with the Brillouin zone boundaries; and, at the same time, the occurrence of "effective zones" in these portions of the Fermi surface is favored as a consequence of the low Fermi velocities near the Brillouin zone boundaries. These considerations suggest that the behavior of the shear wave attenuation by electrons in tin may strongly reflect the influence of interactions attributable to shear deformation of the Fermi surface. Experimental observations in the present work, on the ratio of residual-to-total shear wave attenuation, indicate that this is indeed the case.

It has been noted that the temperature dependence of the superconducting shear wave attenuation, typified by Fig. 1, appears in general to be separable into two regions, a sharp initial decrease of attenuation as temperature falls below T_c and a "residual" attenuation region (labeled "R" in Fig. 1), characterized by a gradual drop of attenuation with decrease of temperature. There is a fairly good understanding of the nearly discontinuous behavior near T_c. Some time ago Morse[12] suggested that the sharply falling attenuation near T_c arises from the "shorting" of the local electric fields associated with the transverse wave as a result of the appearance of superconducting electrons. Tsuneto[19] has found theoretically that this electrodynamic effect should indeed give rise to a rapidly falling interaction which becomes negligible below the immediate region of T_c. Bardeen and Schrieffer[2] have suggested that the region of rapid fall is due to the Meissner effect which results in strong screening of the transverse electric fields by the supercurrents; the transverse particle displacements are associated with transverse currents, and the magnetic field generated by the transverse current is screened in a distance of the order of the penetration depth $\lambda \sim 5 \times 10^{-6}$ cm.

Claiborne[42,43] has studied the shear wave attenuation of aluminum experimentally, giving special attention to the rapid-fall region near T_c, and has derived a theory to describe the attenuation in the rapid-fall region. The results of the calculation are in good agreement with the observed behavior near T_c for his data on aluminum. This calculation uses the London equations to describe the superconducting behavior near T_c, and the method of Holstein cited earlier. The residual attenuation $\alpha_r(T)$, that part of the electronic attenuation lying below the sharp falloff region, is found to be given by

$$\alpha_r(T) = g\alpha_n \cdot 2F(\mathcal{E}), \tag{11}$$

where the symbol "g" is the same one that appeared before, in Eq. (1), Pippard's expression for the normal attenuation. The dependence of g on ql is shown in Fig. 10. The calculation, therefore, predicts that the residual part of the total attenuation will decrease as ql increases. That is, the shorting-out effect should be negligible for very small ql and become more important with increase of ql. In the calculation, the collision-drag effect is entirely responsible for the appearance of a residual attenuation.

In point of fact, the actual situation is expected in general to be more complicated. The presence of a collision-drag contribution to the residual attenuation is independent of the assumption of an arbitrary Fermi surface. In general it must be assumed that there is also a contribution to the shear wave attenuation from "real-metal" effects, by which is meant here electron-lattice interaction which gives rise to a residual attenuation as a result of shear deformation of the Fermi surface. Claiborne found that the experimentally observed

[41] See, for example, Ref. 31 and 32.

[42] R. W. Morse, IBM Res. Develop. 6, 58 (1962).

[43] L. T. Claiborne, Ph.D. thesis, Brown University, 1961 (unpublished).

residual superconducting attenuation in aluminum can be accounted for by the collision-drage effect alone. It is of interest to ask whether this is also the case for tin. Experiment and theory suggest that, unlike the case of tin, the aluminum Fermi surface is relatively simple; only three zones appear to be occupied, and the general shapes of the reduced-zone structures are only very slightly modified from the free-electron topology.[44,45]

If the symbol α_R is introduced to represent the total residual electronic attenuation, i.e., the value of $\alpha_r(T)$ at the highest temperature in the residual region, then Eq. (11) may be rewritten

$$\alpha_R/\alpha_n = g, \qquad (11')$$

where α_R has been defined earlier as the total residual attenuation; $\alpha_r(T)$ is the residual attenuation remaining at temperature T. In the measurements on aluminum by Claiborne the frequency dependence of the ratio α_R/α_n was found to be given rather closely by the quantity g; and, in addition, the g values obtained from these measurements of α_R/α_n were found to be consistent with the frequency dependence of the free-electron expression for α_n given by Eq. (1)

$$\alpha_n = K[(1-g)/g].$$

A summary of the residual attenuation results in the present work on tin is given in Table III.

In Fig. 11 are shown representative attenuation versus temperature data which indicate the regions of sharp falloff and residual attenuation, for two distinct shear wave orientations. The values of α_R/α_n in Table III were obtained by direct measurement of attenuation, while the listed g values were estimated by means of ql determinations from magnetoacoustic measurements. Note that the g values listed are *upper-limit* determinations; g is a monotonically decreasing function of ql (see Fig. 10) and the associated ql values are lower-limit determinations.

TABLE III. The residual superconducting attenuation.

Sample	Orientation and frequency	$\alpha_R/\alpha_n(\pm 0.04)$	$g(ql)$ (upper limit)
I	$q\|\|001$, $\epsilon\|\|100$ 33.5 Mc/sec	0.51	0.20 (max)
I	$q\|\|001$, $\epsilon\|\|100$ 34.7 Mc/sec	0.50	0.19 (max)
I	$q\|\|001$, $\epsilon\|\|100$ 32 Mc/sec	0.52	0.21 (max)
II	$q\|\|100$, $\epsilon\|001$ 10.2 Mc/sec	0.60	0.48 (max)
II	$q\|\|100$, $\epsilon\|\|010$ 10.3 Mc/sec	0.64	0.36 (max)
II	$q\|\|110$, $\epsilon\|\|110$ 10.2 Mc/sec	0.44	0.36 (max)

[44] W. A. Harrison, Phys. Rev. **118**, 1182 (1960).
[45] B. W. Roberts, Phys. Rev. **119**, 1889 (1960).

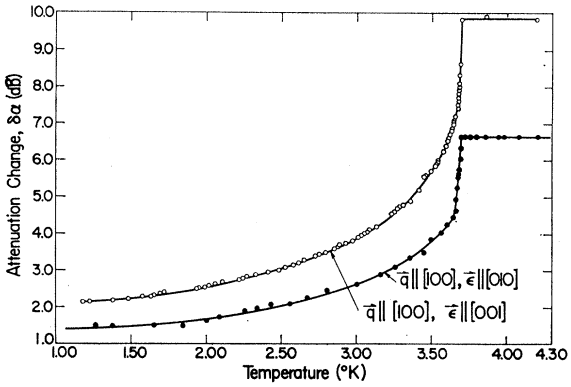

FIG. 11. Temperature dependence of attenuation from 4.2°K to approximately 1.2°K for two distinct shear wave orientations. Frequency is 10 Mc/sec.

It is to be noted that, for all orientations of $\mathbf{q}$ and $\boldsymbol{\epsilon}$ examined, the observed α_R/α_n ratios do not scale with ql according to the free-electron relation, Eq. (11'). In addition, the observed ratios α_R/α_n are consistently greater in magnitude than the g values obtained from the relation $g(ql)$. Finally, it is significant that the disagreement between the measured α_R/α_n and the associated g values becomes considerably smaller at the lower frequency. These observations are consistent with the assertion that, in general, the residual attenuation α_R is determined by effects which include shear deformation as well as collision drag. Since $g(ql)$ increases with decrease of frequency (see Fig. 10), the collision-drag contribution to the residual attenuation, α_R/α_n, is expected to become relatively more important than that attributable to shear deformation as frequency is reduced, and, consequently, the agreement between α_R/α_n and $g(ql)$ to improve. Studies are continuing in a number of superconductors to determine the effect on α_R/α_n of varying electronic mean free path, ultrasonic frequency, and orientation of the shear wave relative to crystalline axes.

IV. CONCLUSIONS

The superconducting attenuation of shear waves in tin has been shown to be consistent, at low reduced temperatures ($t>1.7$), with the BCS prediction,

$$\alpha_s/\alpha_n \propto e^{-\delta/kT},$$

for all principal propagation and polarization orientations.

It has been indicated from measurements of the total and residual electronic attenuation that, in superconducting tin, electron-phonon interaction associated with shear deformation of the Fermi surface contributes significantly to the observed ultrasonic attenuation, and that the effect of collision drag on the residual shear

wave superconducting attenuation is inadequate alone to account for the observations in tin. The interesting observation by Hart and Roberts[46] of the insensitivity of α_R/α_n to change of frequency and the absence of a "rapid-fall" region for given orientations of the shear wave in superconducting gallium ($ql>100$) may perhaps be understood in part in accordance with the considerations of the last section.

Anisotropy in the apparent superconducting energy gap has been demonstrated. It was seen that gap anisotropy can be associated with orientation of shear polarization vector as well as the propagation direction. The apparent limiting energy gap values and corresponding orientations are as follows
$2\mathcal{E}=3.4\pm0.2\ kT_c$ for $\mathbf{q}$ along [001] and $\boldsymbol{\epsilon}$ along [100];
$2\mathcal{E}=3.7\pm0.2\ kT_c$ for $\mathbf{q}$ along [100] and $\boldsymbol{\epsilon}$ along [010];
$2\mathcal{E}=3.3\pm0.2\ kT_c$ for $\mathbf{q}$ along [100] and $\boldsymbol{\epsilon}$ along [001].
It is by no means clear that any deep significance can be attributed to actual numbers associated with the gap anisotropy measurements at the present time. In recent theoretical work of Pokrovskii[34] and Privorotskii[35] an attempt has been made to draw connections between a known, simple variation of the electron distribution on the "effective zone" in k space, and the associated superconducting energy gap anisotropy determined by measurement of the superconducting ultrasonic attention.

ACKNOWLEDGMENTS

I am very grateful to Professor R. W. Morse for a number of stimulating discussions, and for his guidance of the research on which portions of the present work are based. I also wish to thank Professor Charles Elbaum, Professor T. D. Holstein, and Dr. P. G. Klemens for informative conversations. Thanks are also due to Professor A. V. Gold for the use of drawings of sections of the extended-zone free-electron Fermi surface of tin.

APPENDIX A

Numerical values of energy gap and attenuation ratio.[a]

t	T_c/T	$\mathcal{E}(t)/\mathcal{E}(0)$	$\mathcal{E}(t)/kT$[b]	$e^{\mathcal{E}(t)/kT}$	$\alpha_s/\alpha_n=2f(\mathcal{E})$
0.19	4.762	0.99998	9.210	9997.	0.0002
0.21	4.762	0.99986	8.3323	4155.	0.0005
0.24	4.167	0.99945	7.2882	1462.	0.0014
0.27	3.704	0.99860	6.4729	647.5	0.0031
0.30	3.333	0.99709	5.8158	335.5	0.0059
0.31	3.226	0.99641	5.6252	277.3	0.0072
0.33	3.030	0.99472	5.2745	195.2	0.0102
0.35	2.857	0.99255	4.9625	142.9	0.0139
0.37	2.703	0.98984	4.6822	108.0	0.0184
0.39	2.564	0.98655	4.4266	83.65	0.0236
0.41	2.439	0.98261	4.1940	66.29	0.0297
0.44	2.273	0.97540	3.8799	48.42	0.0405
0.47	2.128	0.96649	3.5992	36.56	0.0532
0.50	2.000	0.95572	3.3450	28.36	0.0681
0.53	1.887	0.94295	3.1139	22.51	0.0851
0.56	1.786	0.92801	2.9005	18.18	0.1043
0.59	1.695	0.91074	2.7015	14.90	0.1258
0.62	1.613	0.89093	2.5149	12.37	0.1496
0.65	1.538	0.86837	2.3372	10.35	0.1762
0.68	1.471	0.84279	2.1696	8.755	0.2050
0.71	1.408	0.81387	2.0054	7.429	0.2373
0.74	1.351	0.78119	1.8469	6.340	0.2725
0.77	1.300	0.74423	1.6931	5.436	0.3107
0.80	1.250	0.70228	1.5362	4.647	0.3542
0.83	1.204	0.65435	1.3787	3.970	0.4024
0.86	1.163	0.59898	1.2191	3.384	0.4562
0.89	1.124	0.53382	1.0500	2.858	0.5184
0.92	1.087	0.45466	0.86488	2.375	0.5926
0.95	1.053	0.35213	0.64889	1.913	0.6865

[a] See Ref. 32.
[b] $\epsilon(0)$ is assumed here to have the value of $1.76\ kT_c$.

APPENDIX B

Computation of q values from the elastic constants data

Orientation of q	Orientation of ϵ	ρv^2,[a] in dynes/cm² ($\delta<0.7\%$ at 4.2°K	v, in cm/sec ($\rho_{300°K}=7.279$ g/cm²)	λ(10 Mc/sec) in cm ($\times10^{-2}$)	λ(30 Mc/sec) in cm ($\times10^{-2}$)	λ(50 Mc/sec) in cm ($\times10^{-2}$)	q(10 Mc/sec) in cm^{-1} ($\times10^2$)	q(30 Mc/sec) in cm^{-1} ($\times10^2$)	q(50 Mc/sec) in cm^{-1} ($\times10^2$)
[100]	[100] L	8.260	3.38×10^5	3.4	1.1	0.55	1.8	5.7	8.5
	[001] T	2.694	1.82×10^5	1.8	0.6	0.36	3.5	10.4	17.7
	[010] T	2.823	1.97×10^5	2.0	0.7	0.42	3.1	9.0	15.3
[001]	[001] L	10.310	3.77×10^5	3.8	1.3	0.78	1.6	4.8	8.2
	[100] T	2.689	1.82×10^5	1.8	0.6	0.36	3.5	10.4	17.7
[110]	[110] L	9.878	3.69×10^5	3.7	1.2	0.72	1.7	1.7	8.8
	[110] T	1.271	1.31×10^5	1.3	0.4	0.24	4.8	15.7	26.7
	[001] T	2.702	1.82×10^5	1.8	0.6	0.36	3.5	10.4	17.7

[a] See Ref. 39.

[46] H. R. Hart, Jr., and B. W. Roberts, Bull. Am. Phys. Soc. 7, 175 (1962).